Single filament behavior of microtubules in the presence of added divalent counterions

Nathan F. Bouxsein and George Bachand*

SUPPLEMENTARY INFORMATION

S.1.1 Manning Condensation

In salt solutions, a linear polyelectrolyte with a high charge density will tend to neutralize a fraction of its charge when the electrostatic repulsion energy exceeds the limit of thermal energy. The mechanism by which neutralization is accomplished was described by Manning[1] and referred to as the counterion condensation theory. Here, counterions condense onto the polyelectrolyte until the charged density between adjacent linear charges along the polyelectrolyte chain is reduced below a critical value. The ratio between the Bjerrum length (ℓ_b) and the linear charge spacing (ℓ_0) defines this critical point such that counterions will condense when $\ell_b/\ell_o > 1$ (see schematic 1 below). ℓ_b is simply the separation at which the electrostatic interaction between two elementary charges is comparable in magnitude to the thermal energy scale, i.e. $e^2/(\varepsilon\ell_b) \equiv k_BT$ where e is the elementary charge, ε the dielectric constant, k_B the Boltzmann constant and T the temperature.

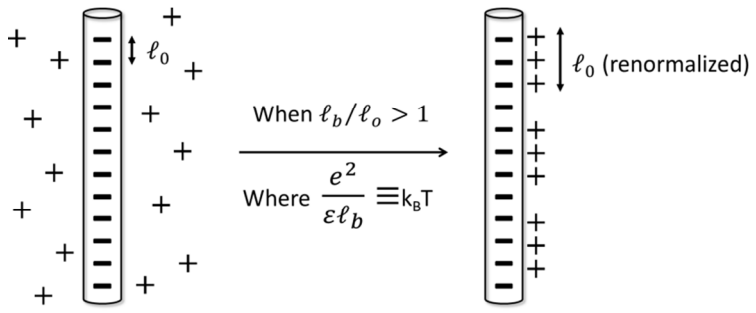

Schematic 1

For a single species of counterions with valence *z*, the fraction of charge neutralization (θ) for a polyelectrolyte due to the presence of the condensed counterions is $\theta = 1 - \ell_o/z\ell_b$. As an example, the fraction of charge neutralization (θ) for DNA in the presence of sodium ions can be estimated to be ~0.76 based on a ℓ_o= 1.7 Å (linear charge spacing, DNA), ℓ_b= 7 Å (in water at room temperature) and z = 1 (valency of a sodium ion). It should be noted here that this theory does not depend on the ion concentration.

In cases where two different ion species ion species are present, specifically where a *z* valent ion is added to a polyelectrolyte dissolved in excess monovalent (*z* = 1) buffer, Manning developed a two-variable solution for determining the fraction of charge neutralization to the polyelectrolyte by each species θ_z and θ_1.[2] These Manning equations were adapted by Wilson and Bloomfield[3] and given by

$$1 + \ln\left(\frac{1000\,\theta_1}{C_1 V_{p1}}\right) = -2\frac{\ell_b}{\ell_o}(1 - \theta_1 - Z\theta_z)\ln\left(1 - e^{-\kappa\ell_o}\right)$$

and

$$\ln\left(\frac{\theta_z}{C_z}\right) = \ln\left(\frac{V_{pz}}{1000e}\right) + Z\ln\left(\frac{1000\theta_1 e}{C_1 V_{p1}}\right)$$

where:

- C_1 and C_z are the molar concentrations of the monovalent and *Z* valent counterions, respectively
- ℓ_o is the charge spacing (for MTs, ℓ_o= 4 Å was assumed)

- κ is the Debye screening length determined by $\sqrt{8\pi\ell_b N_A I}$, where N_A is Avogadro's constant and I is the ionic strength of the solution, which is determined by $\frac{1}{2}\sum C_i Z_i$ where C_i and Z_i are the molar concentration and valence of an ion species in solution, respectively
- V_{p1} and V_{pz} are the volumes in which the condense counterions are considered to be bound locally to the polyelectrolyte, $V_{pz} = 4\pi e N_A(1+Z)(1-Z^{-1})(\ell_o)^3$

The total charge neutralization fraction given in Fig. 5 is thus $\theta_1 + Z\theta_z$. The calculated ionic strength of our control solution (i.e., BRB80) was 180 mM, which includes all components in the buffer, which corresponds to a concentration of monovalent species, C_1 = 129 mM. θ_1 and θ_z were solved simultaneously and numerically in MATLAB for a range of divalent concentrations between C_z = 0.001 and 10 mM and plotted as the dashed line in Fig. 5.

S.1.2 Supplementary Movies

File name: information

SupplementalMovie1.avi : thermal fluctuation of a MT in control monovalent solution, scale bar is 20 µm. Conditions as in Fig. 1.

SupplementalMovie2.avi : thermal fluctuation of a MT in added 5 mM $BaCl_2$, scale bar is 20 µm. Conditions as in Fig. 1.

SupplementalMovie3.avi : sequential images of control MTs in 0.1µM paclitaxel taken at 1 minute intervals highlighting disassembly, scale bar is 20 µm. Conditions as in Fig. 2.

SupplementalMovie4.avi : sequential images of control MTs in 0.1µM paclitaxel and 5 mM $BaCl_2$ taken at 1 minute intervals highlighting disassembly, scale bar is 20 µm. Conditions as in Fig. 2.

SupplementalMovie5.avi : sequential images of control monovalent motility assay taken at 1 second time intervals with 100 ms exposure, scale bar is 20 µm.

SupplementalMovie6.avi : sequential images of added 5 mM $BaCl_2$ to the motility assay taken at 1 second time intervals with 100 ms exposure, scale bar is 20 µm.

SupplementalMovie7.avi : sequential images of control monovalent motility assay highlighting an individual MT transported by kinesin motors. Example phenomenon of MT dispersion and buckling highlighted by arrows and circles respectively. Scale bar is 20 µm. Sequential images are slowed down for effect.

S.1.3 Supplementary Figure 1

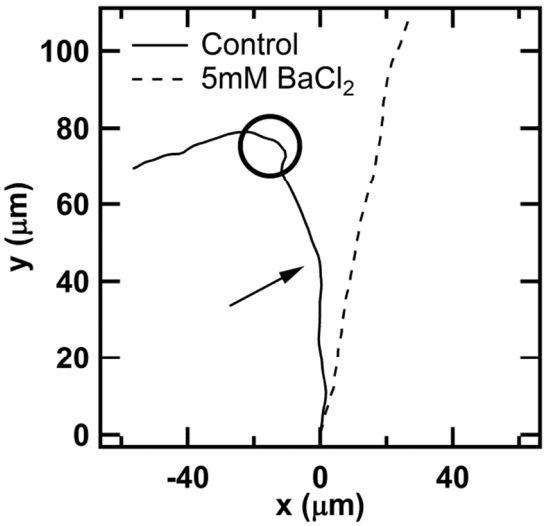

Supplementary Figure 1. MT trajectory comparison. One path trajectory from Fig. 5e (solid line) and Fig. 5f (dashed line) are plotted to highlight the difference in dispersion. The circle in show trajectory deflection when a kinesin motor pins the MT and the arrow shows common deviations that are not apparent in the added salt sample. See supplemental movie Supplemental2C.avi.

S.1.4 Comparison between path persistence with previously reported values

Previous work by Nitta and Hess[4] examined the persistence length of the trajectory path of a population of MT that were binned into groups with no observable pinning or those with pinning. Using a similar cosine regression expression:

$$\langle \cos(\Delta\theta), \Delta t \rangle = \exp\left(-\frac{v_{ave}\Delta t}{2L_{p,path}}\right)$$

where v_{ave} is the average MT velocity, Δt is the time lag and $L_{p,path}$ is the path persistence length, Nitta and Hess measured $L_{p,path}$ = 35 ± 7 µm for pinned MTs and $L_{p,path}$ = 111 ± 20 µm for MT with smooth trajectories.[4] In our control sample (Fig. 5a,c,e) $L_{p,path}$ was estimated at 63.9 ± 10 µm (v_{ave} = 0.68 ± 0.3 µm sec^{-1}) over the entire MT population (pinned and smooth trajectories), which is consistent with the prior results. For 5mM added $BaCl_2$ (Fig. 5b,d,f), $L_{p,path}$ was estimated to be 457.4 ± 40 µm (v_{ave} = 0.70 ± 0.2 µm sec^{-1}), which is approximately four-fold larger than the smooth trajectories previously reported.[4]

S.1.5 Supplementary Figure 2

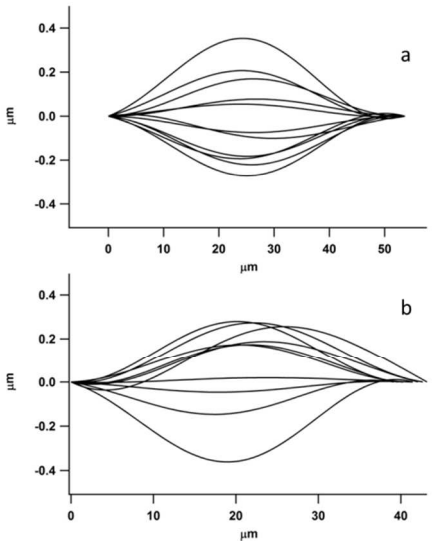

Supplementary Figure 2. Reconstruction of subtilisin treated microtubule shapes. Control shape reconstruction (a) and 5mM added $BaCl_2$ (b) for subtilisin treated microtubules. The shape reconstruction in (a) and (b) is representative of 10 frames from the set of 120 which was re-parameterized into x and y pixel vales, converted into microns based on the microscopes calibration (0.1997 microns/pixel) and rotated by an angle such that the reconstructed filament origin and filament end coincided with the x-axis. The Fourier sums used only the first 3 modes, corrected for the filament intrinsic shape (by subtracting the mean mode amplitudes) for the reconstruction.

S.1.6 References

1. Manning, G. S., *Journal of Chemical Physics* **1969,** *51*, 924-933.
2. Manning, G. S., *Biophysical Chemistry* **1977,** *7*, 95-102.
3. Wilson, R. W.; Bloomfield, V. A., *Biochemistry* **1979,** *18*, 2192-6.
4. Nitta, T.; Hess, H., *Nano Letters* **2005,** *5*, 1337-1342.